Photodynamics of stress in clamped nematic elastomers

Miloš Knežević,[1,*] Mark Warner,[1] Martin Čopič,[1,2] and Antoni Sánchez-Ferrer[3]
[1]*Cavendish Laboratory, University of Cambridge, Cambridge CB3 0HE, United Kingdom*
[2]*Faculty of Mathematics and Physics, University of Ljubljana, Jadranska 19, SI-1001 Ljubljana, Slovenia*
[3]*Institute of Food, Nutrition and Health, ETH Zürich, Schmelzbergstrasse 9, 8092 Zürich, Switzerland*
(Received 26 March 2013; published 17 June 2013)

We describe the complex time dependence of the buildup of force exerted by a clamped photoelastomer under illumination. Nonlinear (non-Beer) absorption leads to a bleaching wave of a significant *cis* isomer dye concentration deeply penetrating the solid with a highly characteristic dynamics. We fit our experimental response at one temperature to obtain material parameters. Force-time data can be matched at all other temperatures with no fitting required; our model provides a universal description of this unusual dynamics. The description is unambiguous since these are clamped systems where gross polymer motion is suppressed as a possible source of anomalous dynamics. Future experiments are suggested.

DOI: 10.1103/PhysRevE.87.062503 PACS number(s): 61.30.−v, 83.80.Va, 61.41.+e, 78.20.H−

I. INTRODUCTION

Unusual properties of liquid crystal elastomers (LCEs) arise from a coupling between the liquid crystalline ordering of mesogenic molecules and the elasticity of the underlying polymer network. Cross-linked networks of polymer chains of a LCE include mesogenic units that belong to either the polymer backbone (main-chain LCE) or side units pendent to the backbone (side-chain LCE) [1]. The shape of a monodomain nematic LCE strongly depends on the temperature-dependent nematic order parameter $Q(T)$. This connection is a consequence of the coupling of $Q(T)$ with the average polymer chain anisotropy. By increasing the temperature of a LCE, $Q(T)$ decreases, which leads to a decrease of the polymer backbone anisotropy. This decrease of anisotropy manifests itself as a uniaxial contraction of the LCE sample.

Mechanical change can be realized also through a change of nematic order by other means. As first shown in LCEs by Finkelmann *et al.* [2], changes can also be achieved by introducing photoisomerizable groups (e.g., azobenzene) into their chemical structure. These structures will be referred to as nematic photoelastomers. By absorbing a photon, azobenzene dye molecules can make transitions, with a quantum efficiency η_t, from their linear (*trans*) ground state to the excited bent-shaped (*cis*) state. While the rodlike *trans* molecules contribute to the overall nematic order, the bent *cis* molecules act as impurities that reduce the nematic order parameter and lower the nematic-isotropic transition temperature. The illumination of photoelastomers causes the reduction of nematic order, which in turn produces a uniaxial contraction of the sample. On switching off the irradiation, the nematic order parameter recovers its initial dark state value, which results in a macroscopic expansion of the sample.

The characteristic time of the mechanical response of the sample is in the rather wide range of milliseconds [3,4] to hours [2,5–8]. To see whether the slow on response in [2] was caused by a slow polymer dynamics of the nematic elastomer or by a slow photoisomerization kinetics, experiments were done [5–7] on clamped photoelastomers. Contrary to the case of the measurements on a freely suspended sample, the clamped setting requires no physical movement of chains in the network. In such settings the sample is fixed at both ends of its longest dimension (along the nematic director). Then, upon irradiation, the sample cannot shrink and a retractive force is exerted on the clamps (see Fig. 1 for an illustration). This force is measured as a function of time until the photostationary state is reached. On switching off the irradiation, the relaxation of the force begins. It was first observed by Cviklinski *et al.* [6] that the dynamics of the nematic order parameter matches the dynamics of the mechanical response, meaning that the rate-limiting process is dominantly the photoisomerization. They also found that their systems display simple exponential processes for the buildup of and decay of force.

Subsequently, it has been shown in other systems [8] that the stress-temperature experimental data for the on process can be approximately fitted to a simple stretched exponential form $\overline{\sigma}_n(t) = 1 - \exp[-(t/\tau_{on})^{\beta_{on}}]$, where $\overline{\sigma}_n(t)$ is the normalized stress exerted on the clamps (stress at time t divided by the photostationary stress) and τ_{on} and $\beta_{on} < 1$ are fit parameters. Similarly, it was found that the normalized stress in the off process can be fitted to the nearly exponential law $\overline{\sigma}_n(t) = \exp[-(t/\tau_{off})^{\beta_{off}}]$, where $\beta_{off} \approx 0.9$. Such a complex dynamical response cannot be attributed (as is usual) to polymer dynamics since we have clamping. In this paper we show that these findings can in fact be successfully described by our simple model of photodynamics and its conversion into stress in clamped nematic elastomers.

According to the Beer law of light absorption, the light propagating in a thick absorbing sample is attenuated at a constant rate. The light intensity at a depth x into the sample is $I(x) = I_0 e^{-x/d_t}$, where I_0 is the incident intensity and d_t is the characteristic penetration depth of a given material due to absorption by *trans* isomers. However, it has been shown that the simple Beer law for light attenuation through the sample containing dye molecules might be inaccurate due to the so-called photobleaching effect [9–12]. This effect is caused by depletion of *trans* isomers, which allows light to penetrate to greater depths than those predicted by Beer's law. If dye molecules that absorbed photons do not return to their *trans* state immediately, the new photons falling on the sample cannot be absorbed in the initial layers and therefore

*mk684@cam.ac.uk

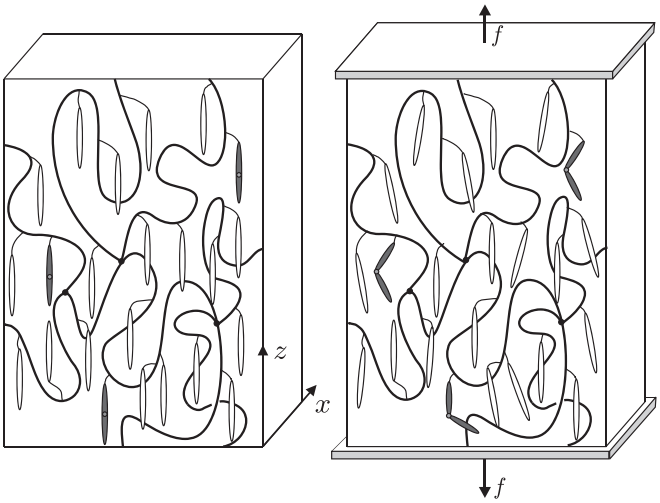

FIG. 1. Schematic of a nematic elastomer with regular mesogenic molecules (white rods) and photoactive molecules (gray). In the dark all photoactive molecules are found in their linear *trans* state (left panel). Upon illumination some photoactive molecules undergo a transition to the bent *cis* state (right panel), which would lead to contraction if the elastomer were freely suspended. Such contraction is prevented by the clamps, resulting in a force f on the clamps.

propagate through the sample following a nonlinear absorption law.

Using the model described in Sec. II, we calculate the stress exerted on the clamps during and after light irradiation. Then we relate the stress to the light absorbance $\mathcal{A} = -\ln(I/I_0)$ at the back of the sample. We apply the full nonlinear absorption model, which takes into account the forward *trans* to *cis* and back *cis* to *trans* photoisomerization as well as thermal isomerization of *cis* molecules back to the *trans* state [11]. The major puzzle in photoactuation is thereby addressed. Beer penetration depths are typically in the 1–10 μm range for normal dye loadings and hence orders of magnitude less than the sample thickness. If a small volume fraction of solid is photocontracted, one expects the overall mechanical response to be small in the Beer limit. We show that the stress is proportional to the *cis* concentration and thus bleaching allows an appreciable sample volume to contribute to the force as a wave of *trans* to *cis* conversion deeply penetrates. To test the validity of our model we fit the on process $\overline{\sigma}_{\rm n}(t)$ data of Ref. [8] at one temperature in order to fix the material constants determining the photoprocesses. The $\overline{\sigma}_{\rm n}(t)$ response at other temperatures then does not need fitting: The same material constants suffice, after they are shifted by the separately measured changes in thermal relaxation times with temperature change, to reproduce the stress response. This remarkable universal agreement between theory and experiment confirms the hypothesis of the domination of photoisomerization over polymer dynamics. We hence explain the observed stretched exponential ($\beta_{\rm on} < 1$) processes in terms of nonlinear spatiotemporal photodynamics rather than the usual (unknown) polymer relaxation processes normally assumed to be behind such complex dynamics. Our analysis reveals that it is important to consider back *cis* to *trans* photoconversion.

II. MODEL

In this section we consider a simple model of stress dynamics of clamped nematic photoelastomers. The resulting stress is calculated within a nematic rubber model in Sec. II A, while the process of nonlinear light absorption is outlined in Sec. II B.

A. Stress exerted on the clamps

Long polymer chains have a Gaussian distribution, becoming anisotropic if they contain mesogenic molecules. The elastic free energy density of a nematic rubber in response to a deformation gradient tensor $\underline{\underline{\Lambda}}$ can be expressed as [1]

$$F = \frac{1}{2}\mu \mathrm{Tr}(\underline{\underline{\ell}}_0 \cdot \underline{\underline{\Lambda}}^{\mathrm{T}} \cdot \underline{\underline{\ell}}^{-1} \cdot \underline{\underline{\Lambda}}) + \frac{1}{2}\mu \ln\left(\frac{\mathrm{Det}(\underline{\underline{\ell}})}{\mathrm{Det}(\underline{\underline{\ell}}_0)}\right), \qquad (1)$$

where $\mu = n_{\rm s} k_{\rm B} T$ is the shear modulus in the isotropic state ($n_{\rm s}$ is the number of network strands per unit volume). The tensors $\underline{\underline{\ell}}$ and $\underline{\underline{\ell}}_0$ generalize the Flory step length, whence directions parallel and perpendicular to the nematic director $\underline{n}$ have values $\ell_\parallel$ and $\ell_\perp$. The matrix $\underline{\underline{\ell}}$ describes the current Gaussian distribution after deformation $\underline{\underline{\Lambda}}$, while $\underline{\underline{\ell}}_0$ gives the initial step lengths. As rubber changes shape at constant volume $\mathrm{Det}(\underline{\underline{\Lambda}}) = 1$. Taking $\underline{n}$ along the z axis, $\underline{\underline{\ell}}$ assumes the diagonal form $\underline{\underline{\ell}} = \mathrm{Diag}(\ell_\perp, \ell_\perp, \ell_\parallel)$. We adopt a simple freely jointed rod model for the polymer backbones, with a step length a in the isotropic state. The elements of $\underline{\underline{\ell}}$ are $\ell_\parallel = a(1 + 2Q)$ and $\ell_\perp = a(1 - Q)$, with Q being the nematic order parameter. Although crude, this model quite accurately describes a wide range of main-chain and side-chain LCEs [1,13]. We will describe side-chain LCE experiments where we envisage the order Q that polarizes the shape of backbone chains as coming from the resultant nematic order of all of the rods: photoinert, *trans*, and *cis*. We are only concerned with derivatives of F with respect to Λ and we shall suppress Λ-independent terms in Eq. (1).

Consider an elastomer in an initial nematic state at temperature T, with $\underline{\underline{\ell}}_0 = \mathrm{Diag}(\ell^0_\perp, \ell^0_\perp, \ell^0_\parallel)$. Illumination changes $\underline{\underline{\ell}}_0$ to $\underline{\underline{\ell}}_{\rm p} = \mathrm{Diag}(\ell^{\rm p}_\perp, \ell^{\rm p}_\perp, \ell^{\rm p}_\parallel)$. A free sample suffers uniaxial spontaneous photodeformation $\underline{\underline{\lambda}}_{\rm p} = \mathrm{Diag}(1/\sqrt{\lambda_{\rm p}}, 1/\sqrt{\lambda_{\rm p}}, \lambda_{\rm p})$ directed along $\underline{n} = \underline{z}$, with its principal contraction $\lambda_{\rm p} < 1$ and perpendicular elongation $1/\sqrt{\lambda_{\rm p}}$ due to incompressibility $\mathrm{Det}(\underline{\underline{\lambda}}_{\rm p}) = 1$. The free-energy density (1) corresponding to $\underline{\underline{\Lambda}} = \underline{\underline{\lambda}}_{\rm p}$ is

$$F = \frac{1}{2}\mu\left(\frac{2}{\lambda_{\rm p}}\frac{\ell^0_\perp}{\ell^{\rm p}_\perp} + \lambda^2_{\rm p}\frac{\ell^0_\parallel}{\ell^{\rm p}_\parallel}\right). \qquad (2)$$

Minimization over $\lambda_{\rm p}$ gives the spontaneous photocontraction $\lambda_{\rm ps} = (\ell^{\rm p}_\parallel \ell^0_\perp / \ell^{\rm p}_\perp \ell^0_\parallel)^{1/3}$. Clearly, $\lambda_{\rm ps} < 1$ since $\ell^{\rm p}_\parallel / \ell^{\rm p}_\perp < \ell^0_\parallel / \ell^0_\perp$, that is, the sample becomes less anisotropic on illumination.

Clamping (see Fig. 1) in effect stretches the sample by $\lambda = 1/\lambda_{\rm ps}$ along $\underline{n}$ to restore the sample to the length before illumination. It is known [13] that strain little perturbs the underlying nematic order. We assume that $\underline{\underline{\ell}}_{\rm p}$ is unchanged after this stretching. Taking $\underline{\underline{\Lambda}} = \underline{\underline{\lambda}} \cdot \underline{\underline{\lambda}}_{\rm ps} = \mathrm{Diag}(1/\sqrt{\lambda\lambda_{\rm ps}}, 1/\sqrt{\lambda\lambda_{\rm ps}}, \lambda\lambda_{\rm ps})$ in (1) and the above value for

λ_{ps}, one gets

$$F = \frac{1}{2}\mu \left(\frac{\mathrm{Det}(\underline{\underline{\ell}}_0)}{\mathrm{Det}(\underline{\underline{\ell}}_p)}\right)^{1/3} \left(\lambda^2 + \frac{2}{\lambda}\right). \quad (3)$$

The result is the same as that of a classical elastomer with a renormalized shear modulus μ. If the formation state were isotropic followed by cooling to a nematic before illumination, F is as in (3) with a different non-light-dependent prefactor [1].

We denote the area of the sample in the nematic state before illumination by A_0 and its length along the director by L_0. Incompressibility gives $A_0L_0 = A_{ps}L_{ps}$, where A_{ps} and L_{ps} are the area and the length of a free sample after illumination. The force exerted by a photoelastomer due to the stretching λ is

$$f = A_0L_0\frac{\partial F}{\partial(\lambda L_{ps})} = A_{ps}\frac{\partial F}{\partial \lambda}, \quad (4)$$

where $A_{ps} = A_0/\lambda_{ps}$. After differentiation, we take $\lambda = 1/\lambda_{ps}$ since there is clamping. The stress $\sigma = f/A_0$ exerted on the clamps takes the form

$$\sigma = \mu \left(\frac{\mathrm{Det}(\underline{\underline{\ell}}_0)}{\mathrm{Det}(\underline{\underline{\ell}}_p)}\right)^{1/3} \left(\frac{1}{\lambda_{ps}^2} - \lambda_{ps}\right). \quad (5)$$

As the shape of the sample is not changing upon the illumination, true and engineering stresses are the same.

The step lengths before illumination are $\ell_\parallel^0 = a[1 + 2Q(T)]$ and $\ell_\perp^0 = a[1 - Q(T)]$. Upon illumination, the *cis* isomers act as impurities that lower the nematic-isotropic transition temperature, which can also be seen as a light-dependent increase of the temperature T [2]. The elements of $\underline{\underline{\ell}}_p$ are $\ell_\parallel^p = a[1 + 2Q(T_{eff})]$ and $\ell_\perp^p = a[1 - Q(T_{eff})]$, where T_{eff} is a fictitious effective temperature that is the actual temperature T increased by a light-dependent term ΔT, whence $T_{eff} = T + \Delta T$. We estimate order change under illumination by taking shift along the $Q(T)$ relation of the dark state. We can examine the effect of *cis* impurities on the free energy. The nematic mean field potential is $U(\theta) = -JQP_2[\cos(\theta)]$, where θ is the angle a rodlike mesogen makes with the nematic director, J is the nematic mean field coupling constant, and P_2 is the second-order Legendre polynomial. The coupling constant J depends on the concentration ρ of linear rods as ρ^ν. The scaling of $J \sim \rho^\nu$ has been argued to have $\nu = 1$ [14,15]. It turns out, however, that our final results will not depend on the specific value of ν. We assume for simplicity that bent *cis* isomers have no nematic order; they weaken the effective potential experienced by the linear rods. One can show that the temperature-dependent part of Landau–de Gennes expansion of the Maier-Saupe [16] free energy has the form $F_L = \frac{1}{2}A_0(T - T^*)Q^2 + \cdots$, where $T^* = J/5k_B$ is the transition temperature; here we have neglected a small contribution to T^* arising from the rubber elastic free energy. Upon illumination, one can view the change of ρ, and thus change of J and T^*, as an effective change in T at constant T^*.

Our nematic photoelastomers contain regular mesogenic molecules and azo dyes that contribute to the nematic order when in the *trans* state. Let ρ_0 denote the total concentration of all mesogenic molecules in the dark state (no *cis* molecules present) and δ the molar fraction of azo dyes. Upon illumination, the total concentration of linear molecules after time t is $\rho(t) = \rho_h + \rho_t(t)$, where $\rho_h = \rho_0(1 - \delta)$ is the concentration of regular mesogenic molecules (constant in time) and ρ_t is that of azo dyes in the *trans* state at time t [$\rho_t(t = 0) = \rho_0\delta$]. Dye molecules in *trans* and *cis* states contribute to the total dye molecules concentration: $\rho_0\delta = \rho_t(t) + \rho_c(t)$, where $\rho_c(t)$ is the concentration of *cis* molecules at time t. Expressed in terms of *trans* $n_t = \rho_t/\rho_0\delta$ and *cis* $n_c = \rho_c/\rho_0\delta$ number fractions, the previous relation becomes $n_t(t) + n_c(t) = 1$. For the total concentration of linear molecules $\rho(t)$, one can write $\rho(t) = \rho_0[1 - \delta + n_t(t)\delta] = \rho_0[1 - n_c(t)\delta]$. Now the coupling constant J becomes $J(t) = J_0[1 - n_c(t)\delta]^\nu \approx J_0[1 - \nu n_c(t)\delta]$ for $n_c(t)\delta \ll 1$. Thus *cis* impurities decrease T^* by $\Delta T = \nu T^* n_c\delta$, which is equivalent to increasing the real temperature to $T_{eff} = T + \Delta T = T + \nu T^* n_c\delta$.

The actual order parameter (upon illumination) at temperature T is then the dark state order parameter $Q(T)$ shifted to $Q(T_{eff}) = Q(T + \Delta T) = Q(T + \nu T^* n_c\delta)$. If T is not too close to the transition temperature T_{ni}, the last expression can be approximated by [6] $Q(T_{eff}) \approx Q(T) + bn_c$, where we have introduced $b \equiv \nu(dQ/dT)T^*\delta < 0$, since $(dQ/dT) < 0$. Linearization leads to a simple stress off dynamics $\overline{\sigma}_n(t) = e^{-t/\tau}$ (to be discussed in Sec. II B), which is compatible with experimental findings. The exact expression for $Q(T_{eff})$ (without linearization) would convert the simple exponential time decay of n_c to a nonexponential time response of $\overline{\sigma}_n$. Such nonlinearity is more pronounced near the transition and has been seen in optical response [15]. On substituting λ_{ps} in Eq. (5) and writing the elements of step length tensors $\underline{\underline{\ell}}_0$ and $\underline{\underline{\ell}}_p$ in terms of the order parameters $Q(T)$ and $Q(T_{eff}) = Q(T) + bn_c$, one gets a cumbersome expression for σ. Keeping only linear terms in bn_c, consistently with linear decay processes, one obtains

$$\sigma = -3b\mu\frac{n_c}{[1 - Q(T)][1 + 2Q(T)]}. \quad (6)$$

The stress σ is of course positive since b is negative. The *cis* number fraction is time and depth dependent $n_c = n_c(x,t)$, which leads to a (x,t) dependence of the stress. To calculate the average stress $\overline{\sigma}(t)$, which is a measure of the force, exerted on the clamps one must integrate over depth $\overline{\sigma}(t) = \int_0^d \sigma(x,t)dx/d$, where d is the sample thickness. To do this, we have to explore the behavior of the *cis* number fraction $n_c(x,t)$.

B. Light absorption

The light intensity I varies with depth x (see Fig. 1) due to absorption by *trans* and *cis* species of dye molecules

$$\frac{\partial I}{\partial x} = -\gamma\Gamma_t I(x,t)n_t(x,t) - \gamma\Gamma_c I(x,t)n_c(x,t), \quad (7)$$

where $\gamma = \hbar\omega\rho_0\delta$ subsumes the energy $\hbar\omega$ of each absorption of a photon from the beam and the absolute number density of chromophores $\rho_0\delta$. Here Γ_t and Γ_c are rate coefficients for photon absorption. We assume Γ to be independent of nematic order. Such feedback would be an additional source of nonlinearity that has been discussed elsewhere [14]. Further, the experiments we shall describe were performed

using unpolarized light, which one can show reduces the sensitivity of Γ to changes in nematic order. We shall find excellent agreement with experiment using this independence assumption.

To simplify the above relation, we normalize $I(x,t)$ by the incident intensity I_0 to obtain $\mathcal{I} = I/I_0$. The combinations $\gamma\Gamma_t$ and $\gamma\Gamma_c$ will be written as $1/d_t$ and $1/d_c$, respectively. Now Eq. (7) becomes

$$\frac{\partial \mathcal{I}}{\partial x} = -\frac{n_t(x,t)}{d_t}\mathcal{I}(x,t) - \frac{n_c(x,t)}{d_c}\mathcal{I}(x,t). \tag{8}$$

Assuming that the *trans* population of absorbers does not change appreciably $n_t(x,t) \simeq 1$, one obtains Beer attenuation $\mathcal{I} = e^{-x/d_t}$. To close Eq. (8) one needs the rate equation for the *trans* population at (x,t),

$$\frac{\partial n_t}{\partial t} = -\eta_t\Gamma_t I(x,t)n_t(x,t) + \left(\eta_c\Gamma_c I(x,t) + \frac{1}{\tau}\right)n_c(x,t). \tag{9}$$

The changes in n_t are due to photoconversions (with quantum efficiencies η_t per photon absorption of *trans* to *cis* transition and η_c per photon absorption of *cis* to *trans* transition) and thermal back reaction from the *cis* population at a rate $1/\tau$, with τ being the *cis* lifetime. Equation (9) can be rewritten as

$$\tau\frac{\partial n_t}{\partial t} = [1+\beta\mathcal{I}(x,t)] - [1+(\alpha+\beta)\mathcal{I}(x,t)]n_t(x,t), \tag{10}$$

where the combinations $\alpha = \eta_t\Gamma_t I_0\tau$ and $\beta = \eta_c\Gamma_c I_0\tau$ measure how intense the incident beam is compared with the material constants $I_t \equiv 1/\eta_t\Gamma_t\tau$ and $I_c \equiv 1/\eta_c\Gamma_c\tau$. The parameter α is the ratio between the forward *trans* to *cis* conversion rate $\eta_t\Gamma_t I_0$ and the thermal back rate $1/\tau$; the parameter β has a similar interpretation. Note that both α and β depend on temperature T since the *cis* to *trans* thermal decay is activated, $\tau = \tau(T)$, and τ is measurable directly or in stress decay.

After integration of Eq. (8) over depth x we get

$$\int_0^d n_c(x,t)dx = \frac{d - d_t\mathcal{A}(d,t)}{1 - d_t/d_c}, \tag{11}$$

where the absorption is determined by the relation $\mathcal{A}(x,t) = -\ln\mathcal{I}(x,t)$. From the above equation one easily obtains the average stress

$$\overline{\sigma}(t) = -\frac{3b\mu}{(1-Q)(1+2Q)}\frac{1-(d_t/d)\mathcal{A}(d,t)}{1-d_t/d_c}. \tag{12}$$

In experiments one usually measures the normalized stress $\overline{\sigma}_n(t) = \overline{\sigma}(t)/\overline{\sigma}_s$, where $\overline{\sigma}_s$ is the stationary state stress

$$\overline{\sigma}_n(t) = \frac{1-(d_t/d)\mathcal{A}(d,t)}{1-(d_t/d)\mathcal{A}(d)}. \tag{13}$$

Here we adopt the convention that $\mathcal{A}(d)$ denotes the steady state value of the absorption $\mathcal{A}(d,t)$. The same convention will be used for $\mathcal{I}$, n_t, and n_c.

For off dynamics, after setting $I = 0$ in Eq. (9), one gets a simple equation for the *cis* number fraction $n_c(x,t) = n_c(x,0)e^{-t/\tau}$, where $n_c(x,0)$ represents the spatial profile of n_c at the instant the light is switched off $t = 0$. On inserting $n_c(x,t)$ into Eq. (6), averaging over depth, and normalizing the average stress with its value at $t = 0$, one gets a simple expression $\overline{\sigma}_n(t) = e^{-t/\tau}$.

Given that the stress $\overline{\sigma}_n(t)$ for on dynamics depends on both $\mathcal{A}(d,t)$ and $\mathcal{A}(d)$, we shall first discuss the behavior of these quantities. In the steady state $\partial n_t/\partial t = 0$ we have

$$n_t(x) = \frac{1+\beta\mathcal{I}(x)}{1+(\alpha+\beta)\mathcal{I}(x)}, \quad n_c(x) = \frac{\alpha\mathcal{I}(x)}{1+(\alpha+\beta)\mathcal{I}(x)}. \tag{14}$$

Now the equilibrium solution of Eq. (8) can be expressed in the form

$$\ln(\mathcal{I}) + \left(\frac{\alpha-\eta\beta}{\beta(1+\eta)}\right)\ln\left(\frac{1+\beta(1+\eta)\mathcal{I}}{1+\beta(1+\eta)}\right) = -\frac{x}{d_t}, \tag{15}$$

where $\eta = \eta_t/\eta_c$ is the ratio of the quantum efficiencies. The above expression for $\mathcal{I}(x)$ provides a generalization of the usual Beer law. Deviations from Beer's law come about because at high intensities the *cis* population increases and is generally less absorbing than the *trans* species. In the limit $\Gamma_c \to 0$, the parameter $\beta \to 0$ so that Eq. (15) reduces to

$$\ln(\mathcal{I}) + \alpha(\mathcal{I}-1) = -\frac{x}{d_t}. \tag{16}$$

For $\alpha = 0$, one finds the standard Beer law $\mathcal{I} = e^{-x/d_t}$, while for large α the law acquires the linear form

$$\mathcal{I}(x) \simeq 1 - \frac{x}{\alpha d_t}, \tag{17}$$

at least over depths up to $x \sim \alpha d_t$ whereupon $\mathcal{I}$ is small and the $\ln(\mathcal{I})$ again prevails to give a finally exponential penetration. The variation of light intensity with reduced depth for large α is represented in Fig. 2 by the solid line $t/\tau = \infty$ in the case of the absence of back photoconversion ($\beta = 0$) and by the dash-dotted line $t/\tau = \infty$ when $\beta \neq 0$. Note that even a moderate value of β (see Fig. 2) has a major impact on the variation of $\mathcal{I}$ with depth. Non-Beer absorption was first explored for dyes in nematic liquid crystals by Statman and

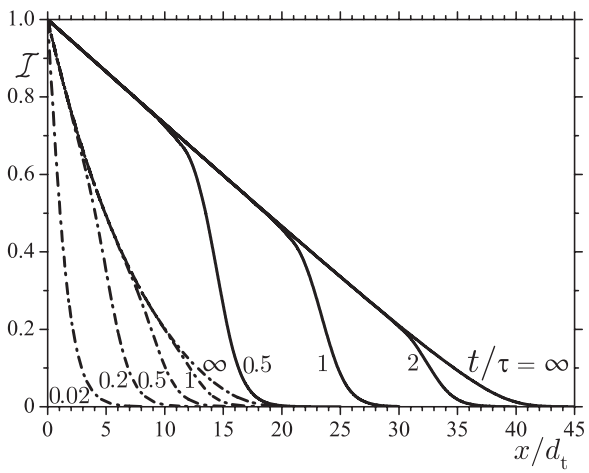

FIG. 2. Light intensity versus the reduced depth x/d_t for various reduced times t/τ. The dash-dotted lines represent the case with the presence of back photoconversion ($\alpha = 36$, $\beta = 1$, and $\eta = 3$ in this example), while the solid lines correspond to the absence of back photoconversion ($\alpha = 36$ and $\beta = 0$); note that even a small value of β (compared to α) significantly affects the variation of $\mathcal{I}$ with depth. In the limit of large t/τ one achieves the stationary regime described by Eq. (15).

Janossy [9] and by Corbett *et al.* [10–12] and experimentally by Serra and Terentjev [17].

Beer absorption has no dynamics since it holds only if the number fraction n_t is unchanging $n_t = 1$. To explore the dynamics of non-Beer absorption, we have to solve the coupled equations (8) and (10). Indeed, using these two equations one gets [12]

$$\tau\frac{\partial\mathcal{A}}{\partial t} = -\mathcal{A} + \frac{x}{d_t} + (\alpha+\beta)(\mathcal{I}-1) + \left(\frac{\alpha}{d_c}+\frac{\beta}{d_t}\right)\int_0^x \mathcal{I}\,dx. \tag{18}$$

Clearly, the absorption $\mathcal{A}$ can be expressed in terms of reduced variables $\tilde{x} = x/d_t$ and $\tilde{t} = t/\tau$. Taking derivative of the above equation with respect to $\tilde{x}$ and using $\mathcal{I} = e^{-\mathcal{A}}$, we get a partial differential equation in $\mathcal{A}(\tilde{x},\tilde{t})$,

$$\frac{\partial^2\mathcal{A}}{\partial\tilde{t}\,\partial\tilde{x}} = 1 - \frac{\partial\mathcal{A}}{\partial\tilde{x}}[1+(\alpha+\beta)e^{-\mathcal{A}}] + \beta(1+\eta)e^{-\mathcal{A}}. \tag{19}$$

We analyze this equation numerically using the boundary condition $\mathcal{A}(0,\tilde{t}) = 0$ and the initial condition $\mathcal{A}(\tilde{x},0) = \tilde{x}$. The results are presented in Fig. 2. As expected, the light intensity decreases with reduced depth more rapidly in the presence of back photoconversion ($\beta \neq 0$, dash-dotted lines) than in the absence of back photoconversion ($\beta = 0$, solid lines). Note that in both cases the stationary regime is reached for moderate values of the reduced time t/τ.

Before proceeding with the analysis of the behavior of the stress, it is tempting to consider briefly the time evolution of the *cis* number fraction $n_c = n_c(\tilde{x},\tilde{t})$. Thus, by taking $\mathcal{I}$ from Eq. (10) and substituting it into Eq. (8), one gets

$$(\dot{n}_c + n_c)\left[1 - n_c\left(1+\frac{\beta}{\alpha}\right)\right]\left[1 - n_c\left(1-\frac{\eta\beta}{\alpha}\right)\right] = [\dot{n}_c'(n_c-1) - n_c'(1+\dot{n}_c)] + \frac{\beta}{\alpha}(\dot{n}_c' n_c - \dot{n}_c n_c'), \tag{20}$$

where for simplicity we used the notation $\dot{n}_c = \partial n_c/\partial\tilde{t}$ and $n_c' = \partial n_c/\partial\tilde{x}$. In the numerical integration of this equation we use the boundary condition

$$n_c(0,\tilde{t}) = \frac{\alpha}{1+\alpha+\beta}\{1-\exp[-\tilde{t}(1+\alpha+\beta)]\} \tag{21}$$

and the initial condition $n_c(\tilde{x},0) = 0$. The quoted boundary condition is obtained by integration of Eq. (10) for $x = 0$. Figure 3 shows n_c as a function of the reduced depth x/d_t for various reduced times t/τ. It seems that the stationary solution, given by the second equation of (14), is reached already for moderate values of the reduced time t/τ.

We estimate the thickness x_c/d_t of the *cis* layer at t/τ by calculating positions of points of the curves from Fig. 3 where second derivatives of n_c over x/d_t change the sign. In the stationary case, this condition can be expressed analytically by taking the second derivative of the second equation of (14) with respect to x/d_t and using (8),

$$(\alpha+\beta)\beta(1+\eta)\mathcal{I}_c^2 + 2(\alpha-\eta\beta)\mathcal{I}_c - 1 = 0, \tag{22}$$

where $\mathcal{I}_c = \mathcal{I}(x_c/d_t)$. Inserting the positive solution of this equation into Eq. (15), we obtain an equation for the stationary value x_c/d_t. In the nonstationary case we proceed numerically. Results for $\alpha = 36$ and $\beta = 0$ and for $\alpha = 36$ and $\beta = 1$ are presented in Fig. 4. In both cases x_c/d_t increases approximately

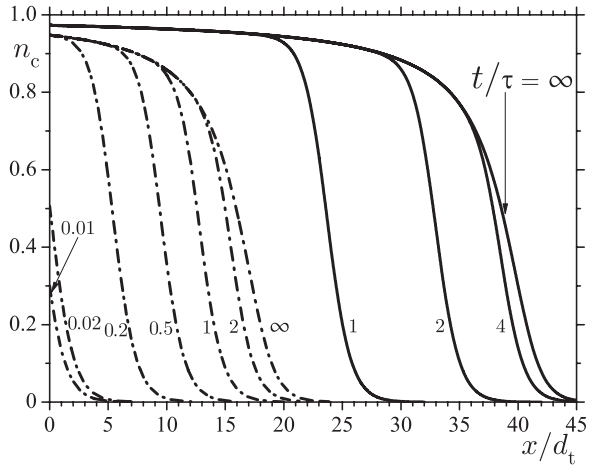

FIG. 3. The *cis* number fraction n_c against the reduced depth x/d_t for various reduced times t/τ. The dash-dotted lines represent the case $\alpha = 36$, $\beta = 1$, and $\eta = 3$, while the solid lines represent the case $\alpha = 36$ and $\beta = 0$. In the large time limit one approaches the solution presented by the second equation of (14).

logarithmically with time in the interval from about 0.5τ to 1.5τ; this can be easily seen if one presents curves from Fig. 4 on a logarithmic scale. The stationary solution is reached in about $t = 4\tau$ for $\beta = 1$ and $t = 5\tau$ for $\beta = 0$. It is also interesting to compare the time needed to reach the stationary state with finite β with the time needed to convert an equally thick layer without *cis* absorption. In Fig. 4 this ratio is about 10, so even though the *cis* absorption is small, it strongly affects the photodynamics of the system. The back photoconversion has also been found to be important in the analysis of experimental findings [18].

III. RESULTS

As we have seen, the absorption $\mathcal{A}$ at the back of the sample $x = d$ in Eq. (13) for stress is actually a function of reduced

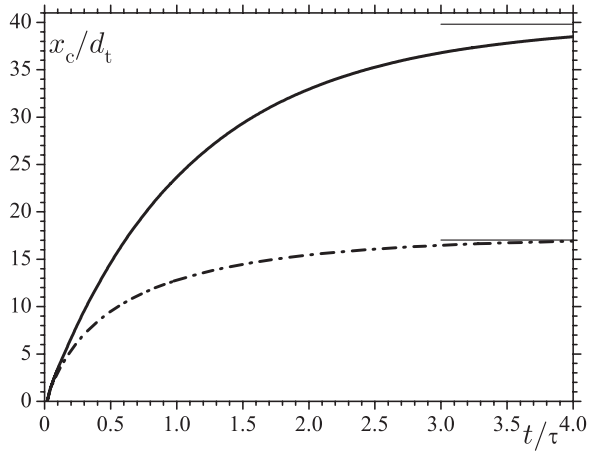

FIG. 4. Approximate thickness x_c/d_t of the *cis* layer against the reduced time t/τ for $\alpha = 36$ and $\beta = 0$ (solid line) and $\alpha = 36$, $\beta = 1$, and $\eta = 3$ (dash-dotted line). Both curves reach their stationary values after a moderate time (measured in units of τ), which coincide with corresponding values (thin solid lines) obtained from Eq. (22) as explained in the main text.

variables $\mathcal{A}(\tilde{d},\tilde{t})$. Then one can generate $\overline{\sigma}_{\rm n}(t)$ for different values of the parameters α, β, $\tilde{d}$, and τ. Experimental data for $\overline{\sigma}_{\rm n}(t)$ were fitted [8] to the simple empirical form $\overline{\sigma}_{\rm n}(t) = 1 - \exp[-(t/\tau_{\rm on})^{\beta_{\rm on}}]$, with $\beta_{\rm on} < 1$. This stretched exponential form must fail at short times and fitting at long times is difficult. We have fitted our theoretical $\overline{\sigma}_{\rm n}(t)$ to the above form. In the absence of *cis* to *trans* photoconversion ($\beta = 0$) we can get fits for $\beta_{\rm on} > 1$ only. If we allow, however, back photoconversion, we can obtain agreement with the stretched exponential form $\beta_{\rm on} < 1$. It is therefore very important to take into account back photoconversion to successfully fit the experimental data.

We consider the experimental data for the compound SCEAzo2-c-10 in Fig. 5(a) of Ref. [8]. There are several quantities entering our relation (13) for stress: the ratio of the quantum efficiencies η, the characteristic thermal relaxation time τ, the thickness of the sample $\tilde{d} = d/d_{\rm t}$ in units of the characteristic length, and the dimensionless parameters α and β. For the ratio of the quantum efficiencies we adopt the estimate $\eta \approx 3$ of Ref. [19]; some larger values of η (up to $\eta \approx 4$) have also been reported. Our analysis shows, however, that the quality of the fit is not very much affected by the particular value of η in the range $\eta \approx 3$–4. For the thermal relaxation times $\tau(T)$ we take the experimental values found in the stress off dynamics [8] $\tau = 51.5$, 33, 23, 15, 10.4, and 7.2 min for temperatures $T = 45\,^{\circ}$C, $50\,^{\circ}$C, $55\,^{\circ}$C, $60\,^{\circ}$C, $65\,^{\circ}$C, and $70\,^{\circ}$C, respectively. With this choice the number of required fit parameters is reduced to three: $\tilde{d}$, α, and β.

We first fit the experimental data for $\overline{\sigma}_{\rm n}(t)$ at $T_0 = 45\,^{\circ}$C to our expression (13), using $\tilde{d}$, α and β as fit parameters (see Fig. 5). The optimal values of fit parameters were found to be $\alpha = 54.9$, $\beta = 1.7$, and $\tilde{d} = 20$. Given that the sample thickness [8] was $d = 300\ \mu$m, the corresponding Beer length is $d_{\rm t} = 15\ \mu$m, which is not far from an independent estimate

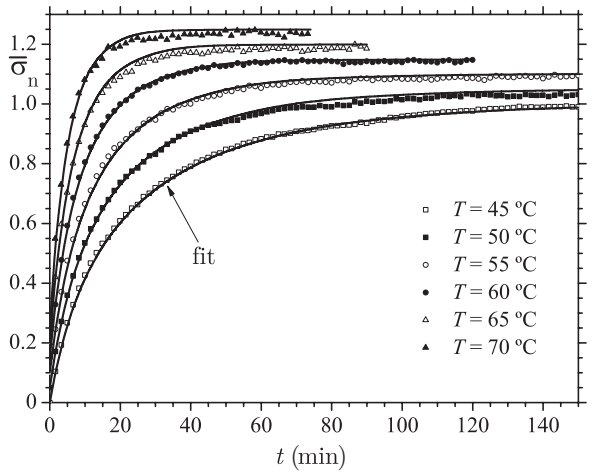

FIG. 5. Normalized stress as a function of time. Theoretical predictions are represented by solid lines, while experimental data, taken from [8], are represented by different symbols corresponding to different temperatures. For better visibility the five curves corresponding to temperatures $T > 45\,^{\circ}$C are shifted along the $\overline{\sigma}_{\rm n}$ axis by the values 0.05, 0.1, 0.15, 0.2, and 0.25, respectively. Only the $T_0 = 45\,^{\circ}$C curve is fitted, while all other curves are theoretical.

$d_{\rm t} \approx 10\ \mu$m obtained from the azobenzene absorption spectra. This rough estimate of $d_{\rm t}$ can be obtained by assuming that the molar extinction for SCEAzo2-c-10 at its absorption maximum coincides with the corresponding known value for the azobenzene in benzene [20]. Let us note, however, that quite good fits can be also obtained for some other values of fit parameters. This ambiguity can be settled obviously by a further reduction of the number of the fit parameters, for example, by measuring $\tilde{d}$. Anyway, in our case the situation is not so serious because the parameter $\tilde{d}$ is temperature independent, while parameters α and β depend on temperature T only through thermal relaxation time $\alpha(T) = \eta_{\rm t}\Gamma_{\rm t} I_0 \tau(T)$ and $\beta(T) = \eta_{\rm c}\Gamma_{\rm c} I_0 \tau(T)$. For example, at other temperatures T, one can write $\alpha(T) = \alpha(T_0)\tau(T)/\tau(T_0)$ and $\beta(T) = \beta(T_0)\tau(T)/\tau(T_0)$. Thus taking the experimental values of thermal relaxation times $\tau(T)$ for temperatures quoted in Fig. 5, we determine the corresponding values of $\alpha(T)$ and $\beta(T)$. Then using these values and expression (13) for the normalized stress, we simply plot corresponding curves for temperatures $T > T_0$ without any fitting. Note the excellent agreement of these theoretical predictions with experimental data. Extracting α and β by fitting at one T_0 gives universal fit-free agreement at other temperatures.

IV. CONCLUSION

We have demonstrated that both significant force magnitude and complex force dynamics result from nonlinear optical absorption. A bleaching wave of increased *cis* concentration, and hence a contribution to retractile force, penetrates a sample with a highly characteristic dynamics in which the (small) absorption of the *cis* moiety is essential. Fitting $\overline{\sigma}_{\rm n}(t)$ at one temperature yields the relevant material parameters of the dye responsible for the optomechanical response. The $\overline{\sigma}_{\rm n}(t)$ response at other temperatures is then obtained with no further fit by simply scaling these parameters by the separately measured decay rates at the other temperatures. This astonishing predictive power indicates the validity of the nonlinear temporal-spatial optical absorption model used.

Future experiments should separately measure Beer penetration depths in the weak absorption limit and the nonlinear material parameters. In that event there should be no fit parameters at all, as in this current work away from the reference temperature. With the material parameters thus measured, one could employ the theory to examine more complex systems such as nonclamped elastomers and systems where the response is more complex due to director patterning.

ACKNOWLEDGMENTS

M.K. acknowledges support from the Winton Programme for the Physics of Sustainability and the Cambridge Overseas Trust and M.W. thanks the Engineering and Physical Sciences Research Council (United Kingdom) for a Senior Fellowship. M.Č. thanks the Winton Programme and Isaac Newton Institute for support. We are grateful to Eugene Terentjev for useful discussions.

[1] M. Warner and E. M. Terentjev, *Liquid Crystal Elastomers* (Oxford University Press, Oxford, 2007).
[2] H. Finkelmann, E. Nishikawa, G. G. Pereira, and M. Warner, Phys. Rev. Lett. **87**, 015501 (2001).
[3] T. J. White, N. V. Tabiryan, S. V. Serak, U. A. Hrozhyk, V. P. Tondiglia, H. Koerner, R. A. Vaia, and T. J. Bunning, Soft Matter **4**, 1796 (2008).
[4] S. V. Serak, N. V. Tabiryan, R. Vergara, T. J. White, R. A. Vaia, and T. J. Bunning, Soft Matter **6**, 779 (2010).
[5] A. R. Tajbakhsh and E. M. Terentjev, Eur. Phys. J. E **6**, 181 (2001).
[6] J. Cviklinski, A. R. Tajbakhsh, and E. M. Terentjev, Eur. Phys. J. E **9**, 427 (2002).
[7] C. L. M. Harvey and E. M. Terentjev, Eur. Phys. J. E **23**, 185 (2007).
[8] A. Sánchez-Ferrer, A. Merekalov, and H. Finkelmann, Macromol. Rapid Commun. **32**, 671 (2011).
[9] D. Statman and I. Janossy, J. Chem. Phys. **118**, 3222 (2003).
[10] D. Corbett and M. Warner, Phys. Rev. Lett. **99**, 174302 (2007).
[11] D. Corbett and M. Warner, Phys. Rev. E **77**, 051710 (2008).
[12] D. Corbett, C. L. van Oosten, and M. Warner, Phys. Rev. A **78**, 013823 (2008).
[13] H. Finkelmann, A. Greve, and M. Warner, Eur. Phys. J. E **5**, 281 (2001).
[14] D. Corbett and M. Warner, Phys. Rev. E **78**, 061701 (2008).
[15] M. Gregorc, H. Li, V. Domenici, G. Ambrožič, M. Čopič, and I. Drevenšek-Olenik, Phys. Rev. E **87**, 022507 (2013).
[16] S. Chandrasekhar, *Liquid Crystals* (Cambridge University Press, Cambridge, 1992).
[17] F. Serra and E. M. Terentjev, J. Chem. Phys. **128**, 224510 (2008).
[18] M. Gregorc, B. Zalar, V. Domenici, G. Ambrožič, I. Drevenšek-Olenik, M. Fally, and M. Čopič, Phys. Rev. E **84**, 031707 (2011).
[19] *Smart Light-Responsive Materials: Azobenzene-Containing Polymers and Liquid Crystals*, edited by Y. Zhao and T. Ikeda (Wiley-VCH, Hoboken, 2009).
[20] http://omlc.ogi.edu/spectra/PhotochemCAD/abs_html/azobenzene.html